https://doi.org/10.22226/2410-3535-2023-1-62-66

Functional properties of NiTi/Kapton nanocomposites deposited by electronic beam evaporation

A. V. Sibirev[†,1], M. V. Alchibaev[1], S. P. Belyaev[1], N. N. Resnina[1], I. A. Palani[2], S. Jayachandran[2], A. Sahu[2]

[†]alekspb@list.ru

[1]Saint Petersburg State University, St Petersburg, 199034, Russia
[2]Indian Institute of Technology Indore, Khandwa Rd, Madhya Pradesh Indore, 453552, India

Shape memory effects were studied in a NiTi/Kapton composite produced by deposition of a thin layer of NiTi on a Kapton substrate by electronic beam evaporation. It was shown that after preliminary deformation by bending at room temperature, the composite demonstrated strain recovery on heating. An increase in preliminary strain increased the recoverable strain the maximum value of which was 2.1%. The two-way shape memory effect was not observed due to a small thickness of the NiTi layer that did not exceed 300 nm. It was shown that the recoverable strain variation on cooling and heating under a stress was not observed due to the polymer creep on heating. The functional properties of the NiTi/Kapton composite produced by e-beam evaporation were compared to the behaviour of the NiTi/Kapton composite produced by the flash evaporation technique. It was shown that the value of the shape memory effect was comparable for both composites, whereas the irreversible strain was smaller in the samples produced by e-beam evaporation.

Keywords: NiTi thin films, shape memory alloys, composite nanofilms, martensitic transformations.

1. Introduction

Shape memory alloys (SMAs) are widely used as working elements for various drives, sensors and actuators due to their unique ability to recover large inelastic strain on heating [1–4]. SMA actuators have several advantages such as higher generated forces, larger strain recovery, smooth and reliable actuation compared to piezoelectric, hydraulics, pneumatics and other traditional actuators [1,5,6]. Also SMAs actuators can be produced in any form factor and easily scalable, thus it makes them to be widely applied in microelectromechanical systems (MEMS) [7–9]. To produce micro SMA drives, different techniques were developed; the main one is the film deposition on a flexible substrate. The polymer substrate serves as support for the SMA layer and plays the role of elastic counter-body. In multiple action actuators, preliminary deformed SMA working body on heating recovers its shape, simultaneously deforming elastic counter-body as a result, the counter-body stores elastic energy on heating and releases it on cooling, while deforming the SMA working body. This cycle can be repeated many times, thus multiple actuation is achieved. Variation of the counter-body stiffness and SMA characteristics allows one to control the actuator parameters [6,10].

There are some deposition methods, that are used to produce SMA thin films: ion sputtering [7,11–13], thermal and flash evaporation [2,8], pulse laser deposition [14]. Recently the electronic beam evaporation technique was used to produce the NiTi/Kapton composite where the thin NiTi layer was deposited to a thick Kapton substrate [15,16]. It was found that the electron beam (or E-beam) evaporation had advantageous over other deposition methods because it allowed one to produce a layer with better uniformity without damaging the underneath polymer substrates [15,16]. This technique provided a higher deposition rate compared to other deposition techniques, which allowed effective varying the thickness of the SMA thin film. Moreover, the E-beam evaporation offered composition control of the deposited thin film and helped in steering the phase transformation temperature of the SMA [15,16].

In [16] it was shown, that the NiTi/Kapton composite produced by e-beam evaporation exhibited the strain variation on thermal cycling without preliminary deformation. However, it is well known that to demonstrate the shape memory effect, the sample should be subjected to preliminary deformation to form the oriented martensite. The disappearance of oriented martensite during the reverse martensitic transformation on heating was the reason for the strain recovery. The larger oriented martensite volume fraction which depended on the pre-strain value, the greater the recoverable strain. Therefore, the standard procedure to study the shape memory effect is the preliminary deformation of the alloy in the martensitic state with the formation of oriented martensite and subsequent heating. In previous studies [15,16], NiTi/Kapton composites were subjected to cooling and heating without pre-deformation in the martensitic state, hence the two-way shape memory effect was studied. At the same time, it is well known that the value of the shape memory effect is larger than the value of the two-way shape memory effect, hence one may assume

that the strain recovery after preliminary deformation will be larger than that found in [16] that may be very attractive for application. Thus, the aim of the present work is to study the peculiarities of strain recovery on heating-cooling-heating of the NiTi/Kapton composite after preliminary deformation by bending.

2. Materials and methods

The NiTi nanofilm was deposited by e-beam evaporation on a Kapton™ polymer substrate with a thickness of 65 ± 3 μm according to the technique described in [16]. Figure 1a shows the view of the NiTi/Kapton composite and in Fig. 1b, a TiNi layer photographed with an optical microscope is presented. After deposition, the thickness of the NiTi layer was measured by scanning electron microscopy and was equal to 300 ± 20 nm. The initial NiTi layer had an amorphous structure, so the samples were held for 2 hours at 350°C in vacuum (10^{-4} bar) for crystallization. Martensite transformations cannot be detected by DSC measurements due to the small mass of the NiTi layer.

To study the functional properties, the samples with a thickness of 65.3 μm, width of 2 mm and length of 40 mm were preliminary deformed by two ways. In the first way, the sample was deformed in the martensite state via bending around the mandrel with a diameter of 2, 1.2, 0.5 or 0.2 mm. During bending, the NiTi layer was on the outer side of the sample and did not touch the mandrel. To calculate the strain after unloading, the sample profile was photographed and digitized with OriginPro™ software as described in [17]. The strain was calculated as $\varepsilon = a/d \cdot 100\%$, where a was sample thickness and d was a bending diameter (Table 1). After preliminary deformation, samples were installed in a holder and subjected to heating-cooling-heating in thermal chamber with a rate of 7°C/min in the temperature range of 120 ÷ 0°C. On temperature variation, the sample profile was photographed and digitized to find the bending radius and calculate the strain. The sample temperature was measured with thermocouple attached to the sample surface. Thus, strain vs temperature dependences were obtained during thermal cycling of NiTi/Kapton composites.

Table 1. Mandrel diameter used for preliminary deformation in martensite and residual strain measured after deformation.

d, mm	2	1.2	0.55	0.2
ε_{res}, %	0.35	0.5	1.1	2.6

In the second way, the one end of the samples was fixed while the mass of 1, 3, 12, 22 or 30 mg were attached to the other end of the sample. This led to the sample bending in cantilever mode. Then sample was subjected to heating-cooling-heating under the stress (produced by the mass m) in thermal chamber. The weight deflection "h" was measured as shown in Fig. 2.

3. Results and discussion

Figure 3 shows the strain variation on thermal cycling of the NiTi/Kapton sample, which was bent around a mandrel with a diameter of 0.55 mm (residual strain was equal to 1.1%). On heating, strain recovery started immediately at room temperature and stopped at 120°C. On further cooling/heating, no strain variation was found. Thus, the NiTi/Kapton sample exhibited the shape memory effect upon the first heating of the pre-deformed sample, but the two-way shape memory effect was not revealed on further thermal cycle. The shape memory effect (ε^{SM}) and irreversible strain (ε^{ir}) values were measured as shown in Fig. 3.

Figure 4 shows the dependences of the shape memory effect and irreversible strain on the residual strain obtained in

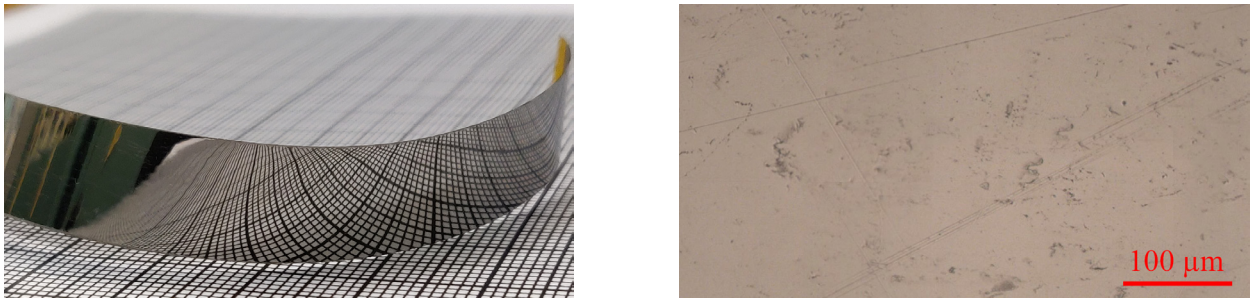

a b

Fig. 1. (Color online) NiTi nanofilm deposited on Kapton by e-beam evaporation. The overall view (a) and TiNi layer surface photographed using optical microscope (b).

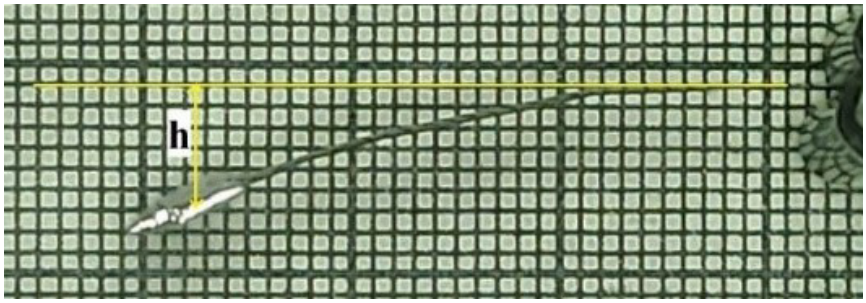

Fig. 2. (Color online) Deflection measurements in NiTi/Kapton composite with a weight attached to one end.

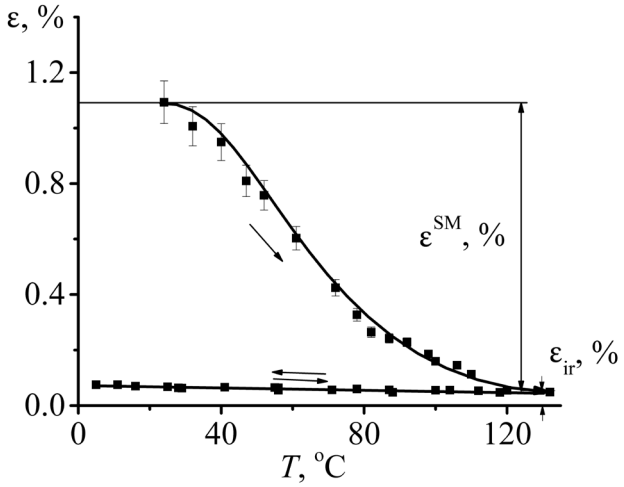

Fig. 3. Strain on temperature variation in the pre-deformed NiTi/Kapton composite deposited by e-beam evaporation.

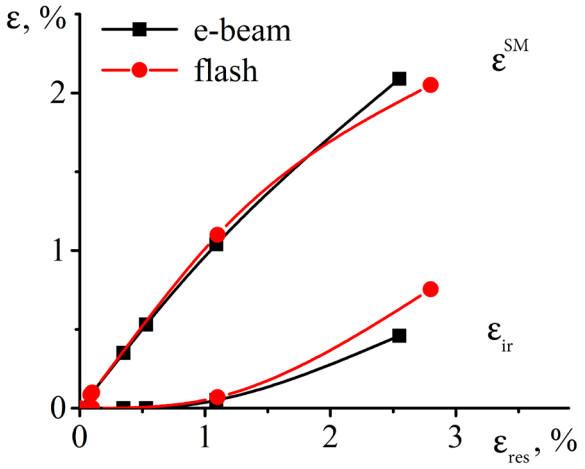

Fig. 4. (Color online) Dependences of the shape memory effect value and irreversible strain on the residual strain obtained for TiNi/Kapton samples deposited by e-beam evaporation (black curves) and by flash evaporation (red curves taken from [17]).

the NiTi/Kapton composites obtained by E-beam evaporation (black curves). As expected, an increase in the residual strain increased the shape memory effect value due to the larger the residual strain, the larger the volume fraction of the oriented martensite, and the larger the shape memory effect value. An increase in residual strain up to 1% did not induce the plastic deformation hence the irreversible strain was equal to zero and all residual strain recovered on heating. An increase in the residual strain over 1%, led to the plastic deformation of the sample, as a result, the recoverable strain decreased, while the irreversible strain increased. The comparison of the results found in the NiTi/Kapton composites obtained by E-beam evaporation (black curves) and by flash evaporation (red curves taken from [17]) showed that the value of the shape memory effect (the recoverable strain) hardly depended on the way for the NiTi/Kapton production. At the same time, the maximum irreversible strain was 0.5% in the NiTi/Kapton composite produced by E-beam evaporation, whereas the same value was equal to 0.8% in the composite produced by flash evaporation. For both cases, the maximum irreversible strain of 2.1% was found in the samples deformed by bending around the mandrel with a diameter of 0.2 mm. After bending the NiTi/Kapton sample around a mandrel with a diameter of less than 0.2 mm, the cracks were found on the NiTi layer surface and adhesion between the NiTi and Kapton layers occurred.

Figure 5a shows the dependence of the composite deflection on temperature found in the TiNi/Kapton composite deposited by e-beam evaporation and subjected to heating-cooling-heating under a mass of 12 mg. It is seen that the deflection increases on the first heating and next cooling. A decrease in the sample deflection was observed on next heating but it linearly depended on the temperature hence it was not included by the martensitic transformation as it was found on heating of pre-deformed sample (see Fig. 3). Variation in the mass attached to the sample affected the value of the strain but did not affect the view of ε(*T*) curves. In all samples, the strain increased during the first heating and next cooling and it linearly decreased on the second heating. It was assumed that an increase in deflection during the first heating under a stress might be attributed to polymer

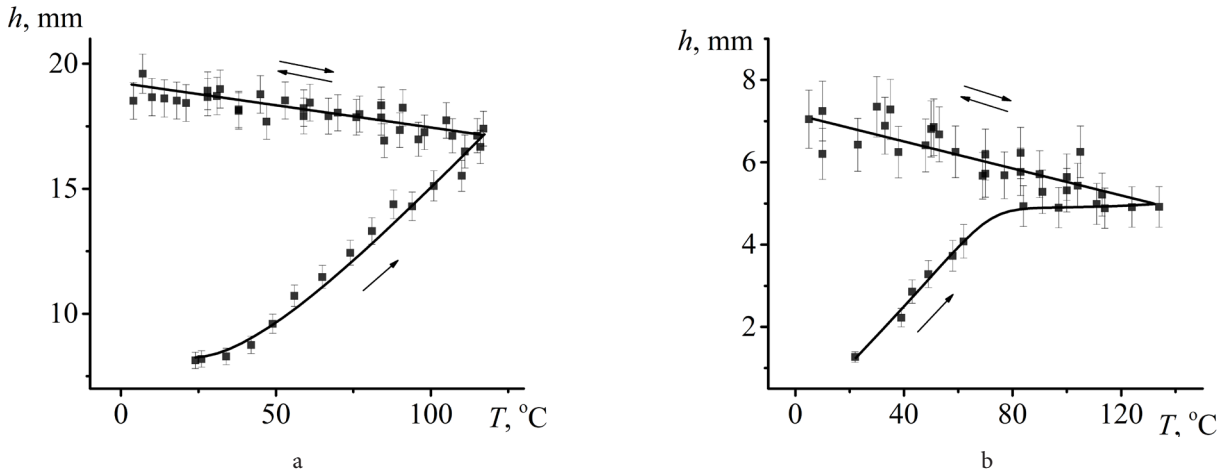

Fig. 5. Variation in the deflection (*h*) on heating-cooling-heating of the NiTi/Kapton composite deposited by e-beam evaporation (a) and for Kapton polymer (b) under a stress induced by a mass of 12 mg.

creep. To investigate this hypothesis, a pure Kapton sample with the same geometrical sizes was subjected to heating-cooling-heating under a mass of 12 mg. Figure 5 b shows that the strain increases on heating and next cooling under a stress in the Kapton sample as it was observed in the NiTi/Kapton composite. Thus, one may conclude that an increase in the strain on the first heating of the NiTi/Kapton composite under a stress was caused by the Kapton creep, whereas the strain variation on further cooling and heating was induced by the difference in the thermal linear coefficients of NiTi and Kapton. The strain variation induced by the martensitic transformation were not found on cooling and heating due to Kapton creep leads to the crack formation in the NiTi layer that upsets the NiTi film integrity.

Thus, the results of the study show that NiTi/Kapton composites produced by the deposition of the NiTi film by e-beam evaporation on Kapton substrate exhibit a shape memory effect after preliminary deformation by bending but they do not demonstrate the two-way shape memory effect.

Thin composite films with a NiTi alloy layer are a difficult object for a study of the functional behaviour, so there are no standard tests. Differences in research methods do not allow comparing the current results with data obtained by other authors. Moreover, most of the authors refuse to calculate the exact values of the recovered strain and use only engineering measurements for their devices (displacements/force values). For instance, in [18] , the microactuators were produced by sputtering a layer of NiTi on a polyimide substrate. It was shown that these microactuators were able to recover the strain after bending, however, the exact dimensions of the sample and the displacements were not pointed out that prevented the calculation of strain. In [19], diaphragm microactuator was obtained by deposition of Ti-Ni thin layer on a Si substrate using the radio-frequency magnetron sputtering method. It was shown that diaphragm exhibited the reasonable actuation on heating/cooling, but recovered strain was not calculated. In [15], electrical actuation of the NiTi/Kapton composite obtained by e-beam evaporation technique was studied. Laser sensor measured displacement of the films edge during Joule heating and 0.9 mm variation in displacement was observed on heating at 3 V, however, strain was not calculated. Moreover, in [15], thin films were studied without heat treatment, while in the present work, the composites were subjected to annealing, that affected the alloy structure that had a great impact to the functional behaviour. In attempt to further improve actuation of NiTi/Kapton composites in [16] the NiTi layer was deposited by e-beam evaporation on a pre-strained up to 3% Kapton layer. Then electrical actuation of the manufactured composites was studied, it was shown that the largest tip displacements of 75 μm were observed for configuration with a 1% pre- strained Kapton layer at 25 V and 0.25 A with a supply frequency of 0.25 Hz, which wasn't a large improvement compared to unstrained sample, which demonstrated 60 μm tip displacement on heating. In current study tip displacement on heating achieved at least several millimeters, however only on the first heating. If the results of the present paper were compared to our previous results [17] where the functional behavior was studied in the NiTi films deposited by flash evaporation method. It was found that both films exhibited similar functional behavior and the maximum recoverable strain was the same. However, the irreversible strain was larger in the samples produced by flash evaporation than in samples obtained by e-beam. It may be due to the difference in the NiTi layer thickness. As it was found in [17], the thickness of the NiTi layer was 500 nm, whereas in the present study, the NiTi layer was a 300 nm thickness. It may be assumed that an increase in the NiTi layer thickness facilitated the dislocation movement and crack formation that increases the irreversible strain.

4. Conclusions

The shape memory effects were studied in the NiTi/Kapton thin composite produced by the e-beam evaporation technique and subjected to crystallization. The following conclusions were drawn:

1. The NiTi/Kapton composite produced by e-beam evaporation exhibits the one-way shape memory effect after preliminary bending in the martensite state, and its maximum value was 2.1%.
2. The NiTi/Kapton composites have not demonstrated the two-way shape memory effect due to a thin NiTi layer was not able to create large internal stresses.
3. The NiTi/Kapton composite was not able to demonstrate the recoverable strain variation on cooling and heating under a stress due to the creep in the Kapton layer on heating under a stress.
4. E-beam evaporation is better for the production of the NiTi/Kapton thin composites because it allows one to obtain samples, which accumulate smaller irreversible strain than the composites produced by flash evaporation.

Acknowledgments. This work was supported by joint DST-RSF project (RSF # 19-49-02014, DST # DST/INT/RUS/RSF/P-36).

References

1. J. Mohd Jani, M. Leary, A. Subic, M. A. Gibson. Mater. Des. 56, 1078 (2014). Crossref
2. E. Makino, M. Uenoyama, T. Shibata. Sensors Actuators, A Phys. 71, 187 (1998). Crossref
3. C. Rossi, D. Lemus, J. Colorado, W. Coral, A. Barrientos. Smart Actuation Sens. Syst. — Recent Adv. Futur. Challenges. InTech (2012). Crossref
4. S. Gopinath, S. Mathew, P. R. Nair. Shape Memory Actuators. In: Actuators. Wiley (2020) pp. 139–158. Crossref
5. S. Hirose, K. Ikuta, K. Sato. Adv. Robot. 3, 89 (1988). Crossref
6. A. Sibirev, S. Belyaev, N. Resnina. Sensors Actuators A Phys. 319, 112568 (2021). Crossref
7. A. Ishida, M. Sato. Thin Solid Films. 516, 7836 (2008). Crossref
8. T. Mineta, K. Kasai, Y. Sasaki, E. Makino, T. Kawashima, T. Shibata. Microelectron. Eng. 86, 1274 (2009). Crossref
9. Y. Fu, H. Du, W. Huang, S. Zhang, M. Hu. Sensors Actuators, A Phys. 112, 395 (2004). Crossref
10. A. V. Sibirev, S. P. Belyaev, N. N. Resnina. Lett. Mater. 11 (2), 209 (2021). Crossref
11. M. Thomasová, P. Sedlák, H. Seiner, M. Janovská,

M. Kabla, D. Shilo, M. Landa. Scr. Mater. 101, 24 (2015). Crossref
12. Y. Kishi, N. Ikenaga, N. Sakudo, Z. Yajima. J. Alloys Compd. 577, S210 (2013). Crossref
13. J.D. Busch, A.D. Johnson, C.H. Lee, D.A. Stevenson. J. Appl. Phys. 68, 6224 (1990). Crossref
14. Y.F. Lu, X.Y. Chen, Z.M. Ren, S. Zhu, J.P. Wang, T.Y. F. Liew. Japanese J. Appl. Physics. 40, 5329 (2001). Crossref
15. S. Jayachandran, S.S. Mani Prabu, M. Manikandan, M. Muralidharan, M. Harivishanth, K. Akash, I.A. Palani. Vacuum. 168, 108826 (2019). Crossref
16. K. Gangwar, S. Jayachandran, A. Sahu, A. Singh, I.A. Palani. Sensors Actuators A Phys. 341, 113607 (2022). Crossref
17. A.V. Sibirev, M.V. Alchibaev, I.A. Palani, S. Jayachandran, A. Sahu, S.P. Belyaev, N.N. Resnina. IOP Conf. Ser. Mater. Sci. Eng. 1213, 012001 (2022). Crossref
18. L. Hou, T.J. Pence, D.S. Grummon. MRS Proc. 360, 369 (1994). Crossref
19. S. Miyazaki, M. Hirano, V.H. No. Mater. Sci. Forum. 394 – 395, 467 (2002). Crossref